Rendezvous revisited: the search for fast-intercept solutions

Anonymous

Department of Physics, Some College, Collegetown, USA

(Dated: April 11, 2022)

Abstract

It is typical of orbital interception scenarios that a chaser is actively maneuvered to intercept and rendezvous with an inertial target, which could be undertaken for a variety of purposes including docking of two spacecraft or collision with an asteroid for planetary defense. The range of viable solutions is constrained by the predetermined trajectory of the target and auxiliary conditions, such as the time to intercept or the fuel budget for the chaser's intercept and rendezvous maneuvers. Whereas a constraint on the time to intercept is central to the Lambert problem, which has been studied extensively, a less common but more visually compelling constraint is a limit on the available fuel for intercept. This was the basis of a recent study [E. M. Edlund, AJP **89**, 559 (2021)], which identified two families of potential intercept solutions. The first family constrains intercept to an integer number of orbits of the chaser while the second family allows for a more general solution with intercept at intermediate points in the orbit. This work concludes this problem by analyzing the second family of intercept solutions and shows that they admit both fast-intercept scenarios and stable solutions.

I. INTRODUCTION

Long before space travel was conceived as a possibility there was great interest in the intercept problem, first made famous by Lambert in 1761. The Lambert problem, as it is now known, seeks the velocity of a body given astronomical measurements of its position at two times because the solution allows the position of the body to be determined at any later time, allowing great predictive capability. This problem spurred seminal developments in celestial mechanics and analysis by some of the best minds of the time.[1,2] There is a long and rich history of literature stemming from the Lambert problem, which was reinvigorated in the 1950's with the development of space programs. This problem lives on in modern incarnations, often with a goal of finding the thrust vector that will allow an actively maneuverable craft to intercept an inertial target at a specific time, because it is mathematically equivalent to the original problem of finding the velocity of an object given information about its position at different times. It is important to note that the general intercept problem can be formulated with constraints other than the time-to-intercept constraint of the Lambert problem, such as intercept given a maximum quantity of fuel.

A number of recent articles have focused on interesting and insight-building problems involving orbital dynamics[3–6]. The first three of these involve, in various ways, the problem of interception, while the latter considers a set of interesting multi-thrust methods for achieving escape velocity from an initially circular orbit. Reference [5] considered a variation on the Lambert interception problem, where the constraint was one of economics rather than time, that is, a constraint on the available. It was argued that this problem presents an excellent challenge for undergraduate students because it requires an intuitive sense of motion on elliptical trajectories, beyond consideration of just the orbital period, and has the allure of game-style challenge of getting one craft to intercept another craft. A simple javascript simulator provided with that article was referenced as a tool for helping to visualize and gamify this study of orbital dynamics.

While the work of Ref. [5] identified two possible families of intercept solutions, it analyzed the intercept and rendezvous problem for only the first family of solutions that occur after an integer number of orbits of the chaser. The second family of intercept solutions is interesting because it allows for intercepts in less than a full orbit. Such fast-intercept maneuvers are relevant to many different situations, involving existential challenges like

planetary defense against civilization killing asteroids or comets where a short, but not predetermined, time may be the essence of the problem.[7] The Planetary Defense Coordination Office, a division within NASA, tracks known threats and develops mitigation plans.[8] As part of that effort, the DART mission is planned to collide with the double-asteroid Didymos in October of 2022 to test deflection by kinetic impact.[9] Other applications of intercept problems include interesting developments like space debris collectors[10] and an actively maneuvering Russian satellite thought to be a satellite hunter of sorts[11].

Analysis of the second family of solutions presents additional challenging and insight-building problems that are within reach of undergraduate students. As in Ref. [5], the methods used here will use graphical representations to identify solutions, which also naturally leads to the idea of solution stability. The equations developed for the second family of solutions are transcendental in nature, and share similarities with analyses from many other subjects, including the motion of projectiles with drag[12], energy eigenvalues in quantum mechanics[13,14], the structure of photonic band-gaps[15], and the propagation of electromagnetic waves[16], among many others. The paper proceeds with some preliminaries and a recap of important results from Ref. [5] in Section II, followed by a formal definition of the problem and derivation of the intercept condition in Section III, with discussion of solutions in Section IV. The final three sections are brief and discuss the sensitivity of solutions in Section V, the rendezvous maneuver in Section VI, and concluding thoughts in Section VII.

II. PRELIMINARIES

Before embarking on a thorough analysis of this problem, the section proceeds by establishing the coordinate system used in this analysis, introduces a few key results for this problem that were established in Ref. [5], and concludes with an examination of a subtle assumption that was made in the analysis of Ref. [5]. Specifically, it was asserted without proof that the Δv for the intercept maneuver was independent of angle, a condition that is not obviously correct considering conservation of energy, which must hold under these conditions.

A. The coordinate system

The analysis presented here uses the definitions and coordinate system that were defined in Ref. [5]. Without loss of generality, the initial motion of both craft is taken to be in the CCW direction. Figure 1 shows the coordinates used to track the target and the chaser, the parameters defining the chaser's thrust vector, the phase of the chaser's elliptical trajectory, and the two families of intercept locations. The first family of possible intercept locations occurs at the origin of motion of the chaser and the second family exists at an angle of 2ϕ from the origin, measured in the CW sense. As in Ref. [5], angles in equations will be expressed in radians, whereas angles in figures will be expressed in degrees to aid with common interpretation.

The angular variables describing the thruster burn of the chaser are the thrust angle, α, which is measured in the CW direction from its "forward" motion, and the magnitude of the thrust. The magnitude of the thrust will always be encountered in the analysis as as a normalized quantity, $\delta = \Delta v/v_0$, where Δv is the change in velocity due to the first thrust maneuver and $v_0 = \sqrt{GM/r_0}$ is the orbital speed for the initial circular trajectory of the target and chaser, with G the universal gravitational constant and M the mass of the central gravitational body. A typical scale for many space missions is $\delta \approx 0.05$, but this can be greatly exceeded in special missions. For example, the third stage of the Saturn V rocket, which propelled the Apollo missions from Earth orbit to the moon, had a δ of order 0.4, and δ's exceeding unity were achieved on the Voyager missions.

In the following, we refer to a "fast-intercept" maneuver, which means interception of the target within one orbit of the chaser. Two predictions for general characteristics of fast-intercept maneuvers emerge from consideration of Fig. 1. First, thrust maneuvers that are directed forward and also somewhat inward, between 270° and 360°, have the tendency to both increase the speed of the chaser and counteract the tendency of the craft to drift toward larger radius, and therefore seem likely candidates for fast-intercept solutions. It is also possible that solutions with some degree of reverse thrust can place the chaser onto a lower altitude orbits that quickly advances its phase relative to the target, and therefore may also provide decently fast solutions. Thus, we expect that fast-intercept maneuvers will require thrust angles between 180° and 360°. Second, it seems intuitive that larger δ should result in smaller time to intercept. Therefore, as the impulse is increased, we anticipate that

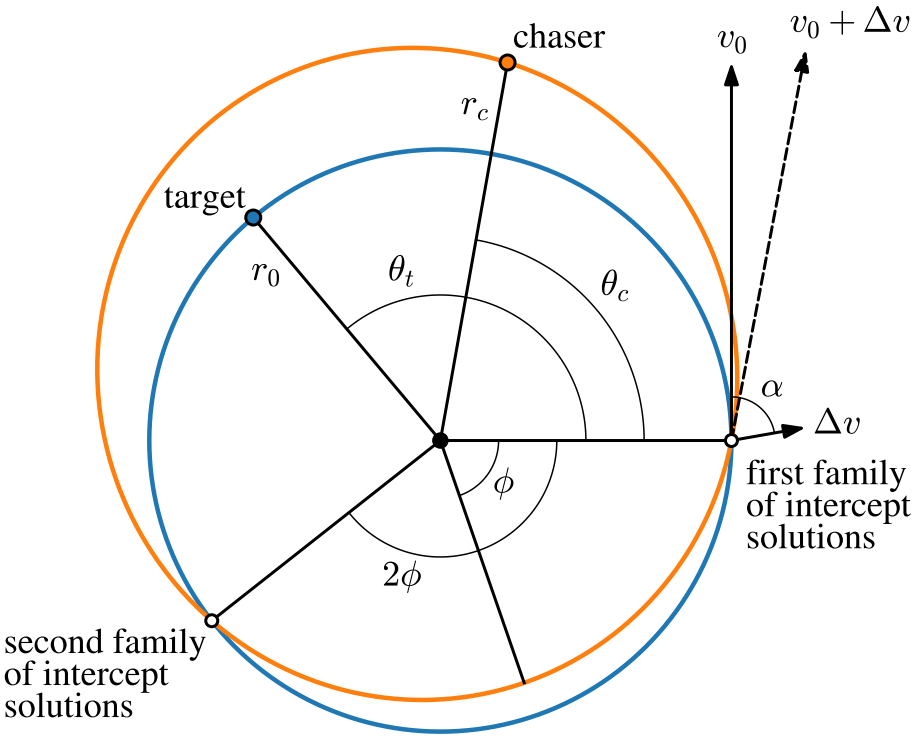

FIG. 1. The coordinate system used in this problem, showing the circular orbit of the target with radius r_0 and angular coordinate θ_t, and the elliptical orbit of the chaser with radius r_c and angular coordinate θ_c. The thrust vector of the chaser shows a Δv at a thrust angle of α, which is measured in the CW sense from the forward direction. The phase angle of the ellipse, ϕ, is measured in the CW sense. The second family of intercept locations is defined by an angular coordinate of $\theta_x = 2\pi - 2\phi$.

the angular coordinate at which intercept occurs should decrease. These predictions will be revisited later in Section IV when the solutions are discussed.

B. The relationship between control parameters and ellipse parameters

Central to this work is a description of the orbital characteristics of the chaser and target on their trajectories. The problem setup begins with the target and chaser initially co-orbital on a circular trajectory of radius r_0 with the target at an initial angular position of θ_0. The target maintains a circular trajectory with radius r_0 at speed v_0 and an orbital

period of $T_0 = 2\pi r_0/v_0$. Following the engine burn that propels the chaser onto its intercept maneuver, it will follow an elliptical trajectory that is described by

$$r_c\left(\theta_c\right) = r_0 \frac{1+\epsilon\cos\left(\phi\right)}{1+\epsilon\cos\left(\theta_c+\phi\right)}, \tag{1}$$

where ϵ is the eccentricity of the elliptical orbit and ϕ is the phase angle of the ellipse. The specific form of Eq. 1 places the chaser at a radius of r_0 at $\theta_c = 0$, as required by the initial conditions. It was also shown how the equation for the chaser's orbital period can be calculated from Kepler's third law by noting that $r_{\text{apogee}} = (1+\epsilon)a$, where a is the semi-major axis of the ellipse. Using Eq. 1 to calculate apogee at $\theta_c + \phi = \pi$, it follows that

$$T_c = T_0 \left(\frac{1+\epsilon\cos\left(\phi\right)}{1-\epsilon^2}\right)^{3/2}. \tag{2}$$

The connection between the ellipse parameters, ϵ and ϕ, and the control parameters, $\delta = \Delta v/v_0$ and α, is not obvious or trivial to derive. Borrowing from the results of Ref. [5], we have

$$\epsilon = \delta\sqrt{\sin^2\left(\alpha\right)\left(1+\delta\cos\left(\alpha\right)\right)^2 + \cos^2\left(\alpha\right)\left(2+\delta\cos\left(\alpha\right)\right)^2}, \tag{3}$$

$$\tan\left(\phi\right) = \tan\left(\alpha\right)\frac{1+\delta\cos\left(\alpha\right)}{2+\delta\cos\left(\alpha\right)}. \tag{4}$$

As point of reference, the extrema of Eq. 4 are $\epsilon = \delta$ at $\alpha = 90^\circ$ and 270°, and $\epsilon = \delta\left(2+\delta\right)$ at $\alpha = 0^\circ$ and 180°. It was shown in Ref. [5] that ϕ has very weak dependence on δ, such that the approximation $\tan\left(\phi\right) = \frac{1}{2}\tan\left(\alpha\right)$ is accurate to within 0.5° for $\delta \leq 0.05$.

C. The assumption of an angle-independent Δv

An interesting conundrum arises when calculating the Δv required for escape from orbit using different thrust directions. When the thrust is applied in the forward direction, that is tangent to the orbit, the Δv required for escape to infinity is equal to $\sqrt{GM/r_0}\left(\sqrt{2}-1\right)$, and when the thrust is applied perpendicularly it is $\sqrt{GM/r_0}$. The principle of conservation of momentum relates the thrust magnitude to a quantity of fuel through the rocket equation, $\Delta v = v_E \ln\left(m_i/m_f\right)$, where v_E is the speed of the engine exhaust and m_i and m_f are the initial and final masses of the rocket, respectively. The fuel required for a given Δv may

be solved by inverting this expression, giving $\Delta m = m_i \left(1 - e^{-\Delta v/v_E}\right)$. This expression indicates that the quantity of fuel, and therefore the chemical energy, required for escape to infinity depends on the path taken. However, in a frictionless system it must also be true that the work required by the engines to get the craft to infinity is a function of only the initial and final positions, and is therefore path independent. We seem to have arrived at a contradiction between conservation of momentum and conservation of energy, which requires a chemical energy that depends on the specific path taken and a work that is path independent, respectively.

Reference [5] took as granted that the Δv for the intercept maneuver should be a constant, that is, independent of α. Yet, in light of the prior arguments, the robustness of this result should be questioned. The conundrum is resolved when it is recalled that it is the total energy that must be conserved, which includes the kinetic energy of the exhaust gases that has hitherto been unaccounted for. In light of this, both of the prior statements are simultaneously true since we accounted only for the work done on the craft. Each path in the escape problem requires a different chemical energy because it requires a different Δv. Applied to the intercept problem considered here, a given quantity of fuel will produce a Δv that is independent of α, but the other orbital characteristics, like the period and kinetic energy of the chaser, will depend on α.

III. DEFINITION OF THE PROBLEM

The two parts of this problem are interception, wherein the chaser arrives at the target, and rendezvous, wherein a second thrust maneuver is performed by the chaser at the time of interception to match velocities with the target. Obviously, the latter process only occurs when some kind of meeting or docking of the two objects is desired, and would not be applicable in the case of intentional collision, as with the DART mission. Of the two parts, the interception problem is the more difficult. That is, once the conditions for intercept are determined, the entire trajectory of the chaser can be calculated and it follows that the derivative of the chaser's position with respect to time then provides the velocity of the chaser at each location. The difference of target's velocity and the chaser's velocity at interception provides the required thrust vector for rendezvous.

The essence of this interception problem is, given a specified Δv, to solve for the thrust

angle that allows the chaser and target be at the same angular coordinate (modulo 2π) and the same radial coordinate at the same time. Unlike the Lambert problem, this formulation puts no constraint on the time to intercept, which is left as a variable in the problem. The approach to finding solutions proceeds as follows: analysis of the radial coordinate is used first to determine the angles at which intercept can occur (Section III A), then the relationship for the angular position of each craft is calculated as a function of time (Section III B). The intercept condition will be derived in Section III C by using the results of the prior parts.

A. The existence of two possible locations for interception

While it is possible to draw an ellipse and a circle that intersect at four locations, in general, the orbits of the chaser and target can intersect at a maximum of two locations because the chaser's orbit is constrained to have the center of force located at one of its foci. The formula that determines the angular locations at which the orbits intersect, defined as θ_x, is found by requiring the radial coordinates of the craft be equal, that is $r_c = r_0$. Using the form of r_c given by Eq. 1 provides

$$\cos(\theta_x + \phi) = \cos(\phi). \tag{5}$$

Two families of solutions emerge from this analysis. The first is the obvious solution that $\theta_x = 2\pi$. It appears, based on the image in Fig. 1 that $\theta_x = 2\pi - 2\phi$ defines the second intersection location. This is indeed a solution to Eq. 5, at least when $\phi < \pi$. The generalization of the second solution to all angles is

$$\theta_x = \begin{cases} 2\pi - 2\phi & 0 \leq \phi < \pi \\ 4\pi - 2\phi & \pi \leq \phi < 2\pi \end{cases}, \tag{6}$$

where $0 \leq \theta_x < 2\pi$. Figure 2 presents the intercept angle plotted as a function of orbital phase angle of the thrust angle, α (solid orange), and the phase of the chaser's elliptical orbit, ϕ (dashed black). When θ_x is plotted as a function of α, the shape of that curve depends on δ through Eq. 4, though it must be recalled that ϕ has a very weak dependence on δ and therefore the shape presented in Fig. 2 is representative of a broad range of thrust magnitudes.

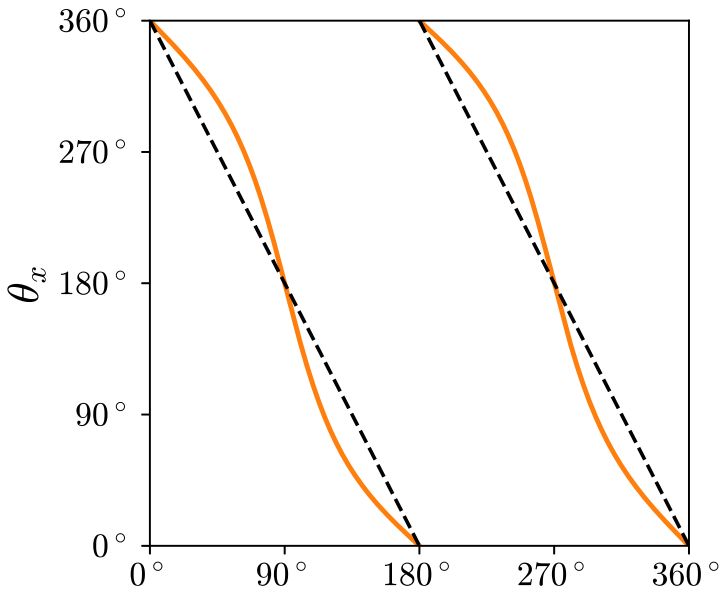

FIG. 2. The intersection angle of the two orbits, θ_x, is plotted against ϕ (black dashed) and α (solid orange), for the case of $\delta = 0.20$.

B. The equations of motion

The intercept condition emerges from the requirement that both craft arrive at an intersection of the orbits at the same time, which requires the equations of motion of both craft. The motion of the target craft is rather straightforward given that it travels on a circular orbit at constant angular velocity $\omega_0 = v_0/r_0$. It follows that the angular coordinate of the target, θ_t, which starts at an initial angle of θ_0, evolves in time as

$$\theta_t\,(t) = \theta_0 + \omega_0\,t. \tag{7}$$

The description of the angular position of the chaser as a function of time can be derived from the constancy of the specific angular momentum, that is, $r_c^2\,\dot{\theta}_c = l_c$. Applied just after the engine burn has completed, before the chaser has changed its position appreciably, we have $l_c = r_0\,v_0\,[1 + \delta\cos(\alpha)]$. Using a variation of Eq. 13 from Ref. [5], $(1 + \delta\cos(\alpha))^2 = 1 + \epsilon\cos(\phi)$, the specific angular momentum may be expressed as $l_c = r_0\,v_0\,(1 + \epsilon\cos(\phi))^{1/2}$. Using this last form for the constant of motion with the expression for $r_c\,(\theta_c)$ from Eq. 1, the differential equation describing the evolution of the chaser's angular position takes the form

$$r_0^2 \left(\frac{1 + \epsilon \cos(\phi)}{1 + \epsilon \cos(\theta_c + \phi)} \right)^2 \frac{d\theta_c}{dt} = r_0 \, v_0 \left[1 + \epsilon \cos(\phi) \right]^{1/2}. \tag{8}$$

After dividing by $r_0^2 \left[1 + \epsilon \cos(\phi) \right]^{1/2}$, separating variables, and integrating between the initial and final states, we have

$$\left(1 + \epsilon \cos(\phi) \right)^{3/2} \int_0^{\theta_c} \frac{d\theta}{\left(1 + \epsilon \cos(\theta + \phi) \right)^2} = \omega_0 \, t. \tag{9}$$

The angular position of the chaser now appears as the upper limit of the integral in Eq. 9. Further progress requires that this integral be evaluated for specific cases. This can be done either by direct numerical calculation or through evaluation of an analytic expression.[3,17] Defining the LHS of Eq. 9 as $I(\theta_c; \epsilon, \phi)$, the analytic expression is

$$I(\theta_c; \epsilon, \phi) = \left(\frac{1 + \epsilon \cos(\phi)}{1 - \epsilon^2} \right)^{3/2} \left[q(\theta_c + \phi) - q(\phi) \right] \tag{10}$$

where we have defined a new quantity, q, given by

$$q(z) = \psi(z) - \epsilon \sin\Big(\psi(z) \Big), \tag{11}$$

with

$$\psi(z) = 2 \tan^{-1} \left(\sqrt{\frac{1 - \epsilon}{1 + \epsilon}} \tan\left(\frac{z}{2} \right) \right). \tag{12}$$

While simpler than Eq. 9 in that no integral needs to be calculated, Eqs. 10-12 obscure the meaning of the expression and are rather complicated in their own. Care must be taken to enforce continuity in ψ as the inverse tangent function passes from $+\pi/2$ to $\pi/2$, which happens as the argument of the tangent function passes through π. In the following sections, the LHS of Eq. 9 is described only as $I(\theta_c; \epsilon, \phi)$ so that readers may use their preferred representation.

C. The intercept condition

An expression for θ_t in terms of θ_c is achieved by substituting the LHS of Eq. 9 for $\omega_0 \, t$ in Eq. 7. The mathematical statement of the intercept condition is finally realized when it is also required that $\theta_t = \theta_c$, modulo 2π, which can only occur at the intersection

locations defined by θ_x in Eq. 6. While a general solution that is applicable to any number of orbits is desired, it is both conceptually simpler and more germane to the problem of fast intercept maneuvers to limit the first analysis to interception within one orbit. Under these conditions, the intercept condition is

$$\theta_x \stackrel{!}{=} \theta_0 + I\left(\theta_x; \epsilon, \phi\right), \tag{13}$$

where the $\stackrel{!}{=}$ symbol is used as a reminder that this is a condition that we want to be true, not one that must be true. Since it is easy to lose the meaning of equations in the process of merging them, we briefly pause to consider how Eq. 13 should be interpreted before moving on. The origin of Eq. 13 is in Eq. 7, which describes the angular position of the target as a function of time. The integral expression $I\left(\theta_x; \epsilon, \phi\right)$ on the RHS represents the the time (properly $\omega_0 t$) required for the chaser to travel to θ_x. Therefore, the RHS represents *the actual angular position of the target when the chaser is at* θ_x and the LHS represents *the goal of having the target at the specific angular coordinate of the intersection of the orbits.*

To generalize Eq. 13 to multiple orbits of the chaser and the target, two things must be done: the extra time required for multiple orbits of the chaser must be accounted for and the target's actual angular position must allow for multiple orbits. The chaser's position enters through θ_x on the RHS of Eq. 13. That is, θ_x should be replaced with $2\pi n_c + \theta_x$, where n_c counts the number of whole orbits of the chaser. To simplify this expression, we use the fact that the integrand of I is periodic in θ to separate the whole-orbit part of the motion as $I\left(2\pi n_c + \theta_x; \epsilon, \phi\right) = I\left(2\pi n_c; \epsilon, \phi\right) + I\left(\theta_x; \epsilon, \phi\right)$. The whole-orbit component of I represents $n_c \omega_0 T_c = 2\pi n_c T_c / T_0$. Using the expression for the period of the chaser's elliptical orbit provided in Eq. 2, it follows that $I\left(2\pi n_c; \epsilon, \phi\right) = 2\pi n_c \left(\frac{1+\epsilon\cos(\phi)}{1-\epsilon^2}\right)^{3/2}$. To complete the generalization of the intercept condition to multiple orbits, we must recall that Eq. 13 is true only modulo 2π. Equivalent to analysis modulo 2π, an integer multiple of 2π can be added to the LHS of the intercept condition to account for multiple orbits of the target. It follows from the prior that the generalized intercept equation is

$$\theta_x + 2\pi n_t \stackrel{!}{=} \theta_0 + 2\pi n_c \left(\frac{1 + \epsilon\cos\left(\phi\right)}{1 - \epsilon^2}\right)^{3/2} + I\left(\theta_x; \epsilon, \phi\right), \tag{14}$$

where n_t counts the number of times the target has passed through $\theta = 0$. That this is the most general statement of the intercept condition for this problem can be seen by noting

that limiting the solution space to $\theta_x = 0$ eliminates the first term on the LHS and the last term on the RHS of Eq. 14, which reproduces the first family of intercept solutions that is described by Eq. 18 of Ref. [5].

IV. SOLUTIONS FOR THE SECOND FAMILY OF INTERCEPT LOCATIONS

Before delving into the search for intercept solutions, it is important to consider the meaning of Eq. 14. Phrased as a question, it asks "For what values of θ_x is this condition true?" It should be expected that the two sides of this expression will rarely be equal, and it is only those rare occasions where they are equal that identify solutions to the intercept problem.

Equation 14 is a transcendental expression for θ_x, which exhibits substantial complexity because ϵ and ϕ are functions of α and δ through Eqs. 3 and 4, respectively. Similar to many other analyses of problems involving transcendental equations, we approach the solution of this problem through a graphical analysis wherein the LHS and RHS of the equation are plotted separately and solutions are identified by the crossings of these curves.[12–16] Figure 3 presents a series of solutions calculated for a range of δ for the special case of $n_t = n_c = 0$, and therefore represent a range of fast-intercept maneuvers admitted by Eq. 14. The thin blue curves in Fig. 3 represent the RHS of Eq. 14, and therefore should be interpreted as the position of the target when the chaser is at the intersection of the orbits, which is represented by the thick orange lines. The discontinuity at $\alpha = 180^\circ$ arises because there is a large change in the intersection angle around this value. For example, considering the case of $\theta_0 = 15^\circ$ and $\delta = 0.2$, we find that θ_x occurs at 0.8° for $\alpha = 179^\circ$ whereas θ_x occurs at 359.1° for $\alpha = 181^\circ$.

We now consider some of the trends in the solution space of the cases shown in Fig. 3. The calculations shown in Fig. 3 show that all fast-intercept solutions require $\alpha > 180^\circ$ and that larger values of δ achieve intercept more quickly under these conditions, in agreement with the predictions asserted in Section II A. To help develop a deeper understanding of the meaning of these curves, it is also useful to consider why other thrust maneuvers do not allow interception. The largest differences between the orange and blue curves of Fig. 3 exist in the the range of of 0° to 90° and 180° to 270°, roughly. Thrust angles in the lower range take the chaser outward and onto larger period orbits. Recalling that the blue curves

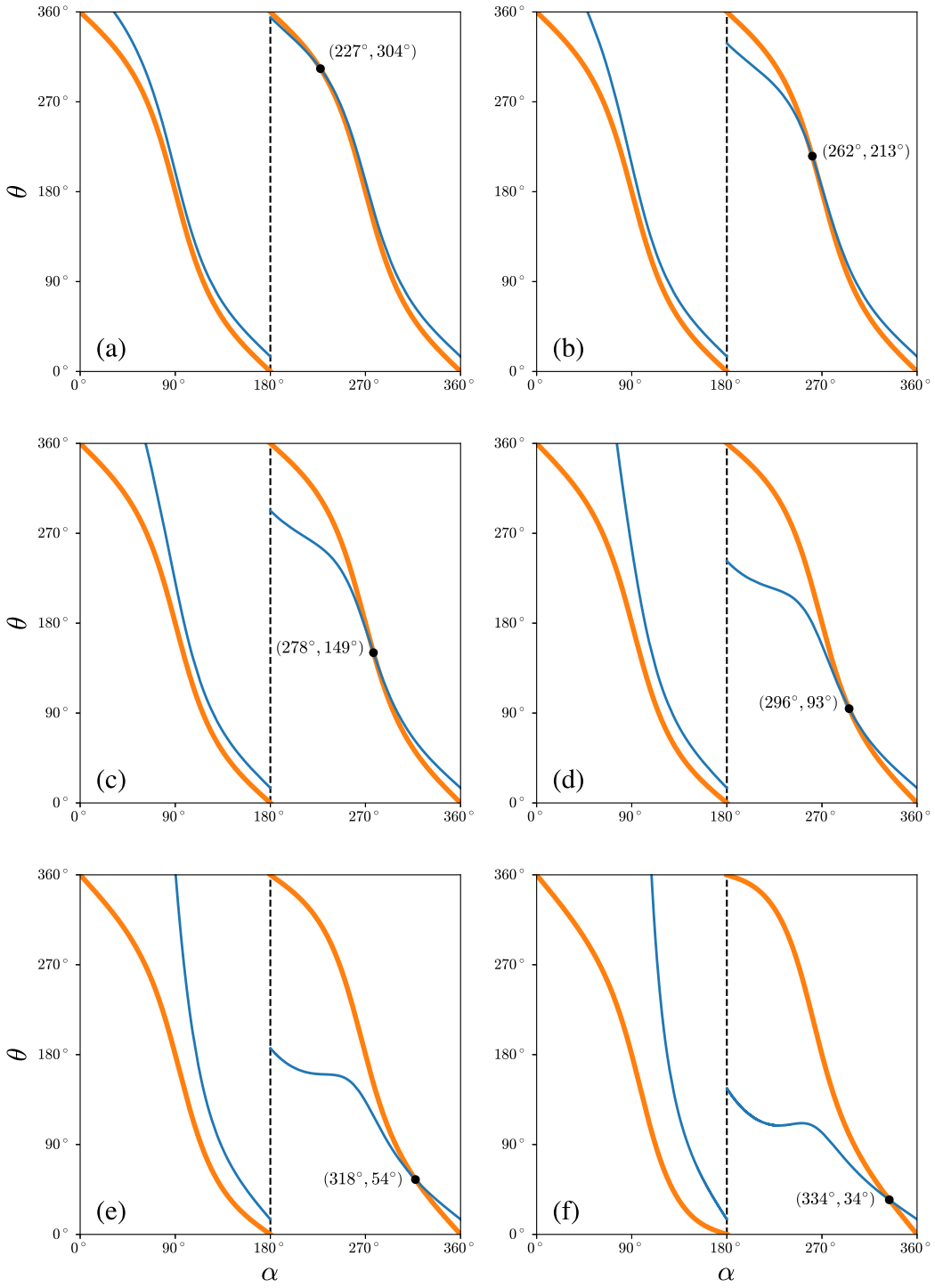

FIG. 3. This series of panels presents fast-intercept solutions for $n_c = n_t = 0$ for a range of δ. The angular position of the target is represented by the thin blue lines and the thick orange lines can be interpreted as the position of the chaser. Case (a) depicts $\delta = 0.02$, (b) depicts $\delta = 0.05$, (c) depicts $\delta = 0.10$, (d) depicts $\delta = 0.20$, (e) depicts $\delta = 0.40$, and (f) depicts $\delta = 0.80$, which collectively show the movement of the intercept angle toward smaller angular positions as δ is increased.

represent the position of the target, their steep rise in the 0° to 90° range, especially for the larger δ cases, should be interpreted as a result of the chaser completing long-period orbits which allows the target's position to evolve toward large absolute angles. Indeed, for $\delta \geq \sqrt{2} - 1 \approx 0.41$ the chaser launches onto unbound orbits for some range of thrust angles. Clearly, these are not viable candidates for fast-intercept maneuvers. In the opposite sense, the large difference between the orange and blue curves in the range of 180° to 270° for larger values of δ comes about because these maneuvers propel the chaser onto significantly lower altitude orbits that rapidly advance its angular position and place it well beyond that of the target when it reaches the intersection location.

Thus far, the analysis has presented the full range of possible thrust angles for specific values of δ. However, it is also useful to consider only the intercept solutions as a function of δ. Figure 4 shows the solution space of α and θ_x that arise for a range of δ, again considering only fast-intercept maneuvers with $n_c = n_t = 0$. A few important points emerge from this view of the problem. The existence of a minimum speed for a fast-intercept maneuver within one orbit is demonstrated by the minimum value of δ below which there are no solutions. Furthermore, this analysis further confirms that fast-intercepts are enabled by thrust angles which tend to be directed forward and inward, in the range of 270° to 360°, approximately. The dashed line in Fig. 4 is the approximate solution for α that would be expected in the limit of a straight-line trajectory for the chaser, which is applicable in the limit of high-speed maneuvers. This approximate form suggests that for $\theta_0 \leq 15°$ and $\delta > 0.5$ the intercept problem becomes decently approximated by linear motion.

Figure 5 illustrates the solution space for the generalized intercept condition of Eq. 14 that admits solutions for multiple orbits of the chaser and target. As before, the LHS of Eq. 14 is represented by the thick orange curves and the RHS is represented by the thin curves, with different values of n_c distinguished by color. It is important to note that the discontinuities in the curves representing the RHS of Eq. 14 disappear when the curves for different values of n_c are added. Though the presentation of the intercept condition becomes considerably more complex when considering multiple orbits, the method for identifying solutions remains the same and it is apparent that a wide range of intercept solutions are possible.

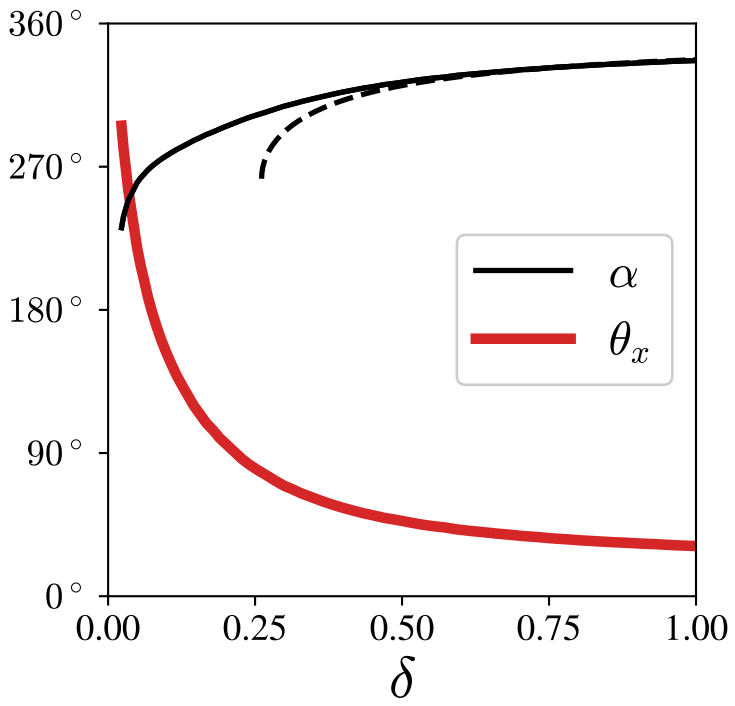

FIG. 4. The value of the thrust angle required for intercept (α) and the intercept angle (θ_x) are plotted as a function of δ for the case of $\theta_0 = 15°$. The dashed line is the approximate solution for α that is arrived at by considering straight line motion (no gravitational force), which shows that for values of δ above about 0.5 there is little difference between the approximate and actual solutions for these conditions.

V. SENSITIVITY TO CONTROL PARAMETERS

An interesting point was made in the work of Ref. [5] that intercept solutions in the vicinity of $\alpha = \pm 90°$ are relatively unstable with respect to perturbations in α, and that stable solutions for the first family require $\alpha = 0°$ or $\alpha = 180°$. An insight into this result can be found in the expression for the orbital period given by Eq. 2, which shows that $T_c = T_0$ when $\cos(\phi) = -\epsilon$. There is no corresponding simple relationship involving α and δ as representation in those variables involves an equation that is cubic in both $\cos(\alpha)$ and δ. For small thrust values, $T_c = T_0$ occurs for ellipse phase angles slightly larger than 90°. This means that small changes in the thrust direction can change the orbital period by only a very small amount, requiring a large change in δ to compensate and ensure interception. This is kind of the opposite of stability and represents extreme sensitivity to control parameters.

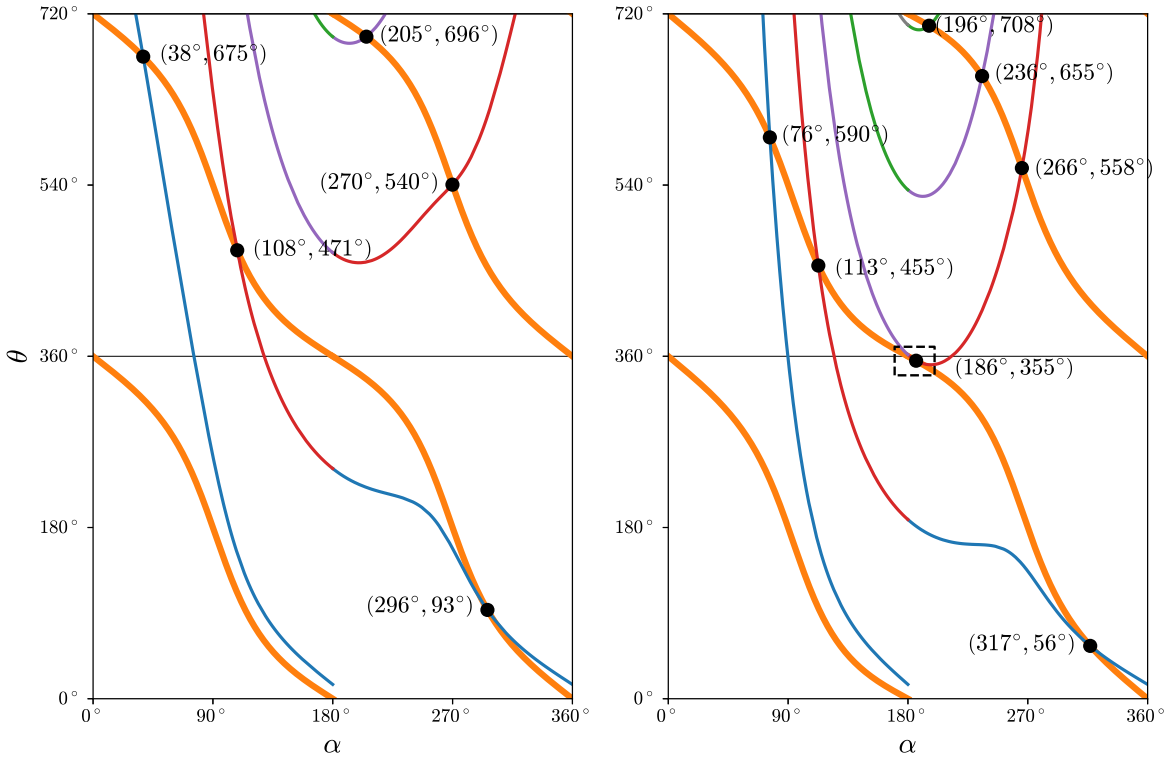

FIG. 5. The left panel shows all intercept solutions for $\delta = 0.20$ and up to two orbits of the target. The right panel shows the same but for $\delta = 0.39$. The thick orange curves represent the LHS of Eq. 14 and the thin curves represent the RHS, with blue representing $n_c = 0$, red representing $n_c = 1$, purple representing $n_c = 2$, green representing $n_c = 3$, and gray representing $n_c = 4$ (just barely visible at the top of the plot on the right). The boxed region around $\alpha = 186°$ is expanded in Fig. 6.

The concept of stability was formalized by considering derivatives of the intercept condition with respect to α. With the first family of intercept solutions it was rather straightforward to prove mathematically that stable solutions exist because it was clear that the RHS of the intercept condition (the equivalent of our Eq. 14) must have points that were tangent to the LHS, which were defined by zero derivative, and it was easy to see how δ could be chosen to ensure interception at those points of tangency. However, it is not obvious whether stable solutions exist for the second family of intercept solutions because of

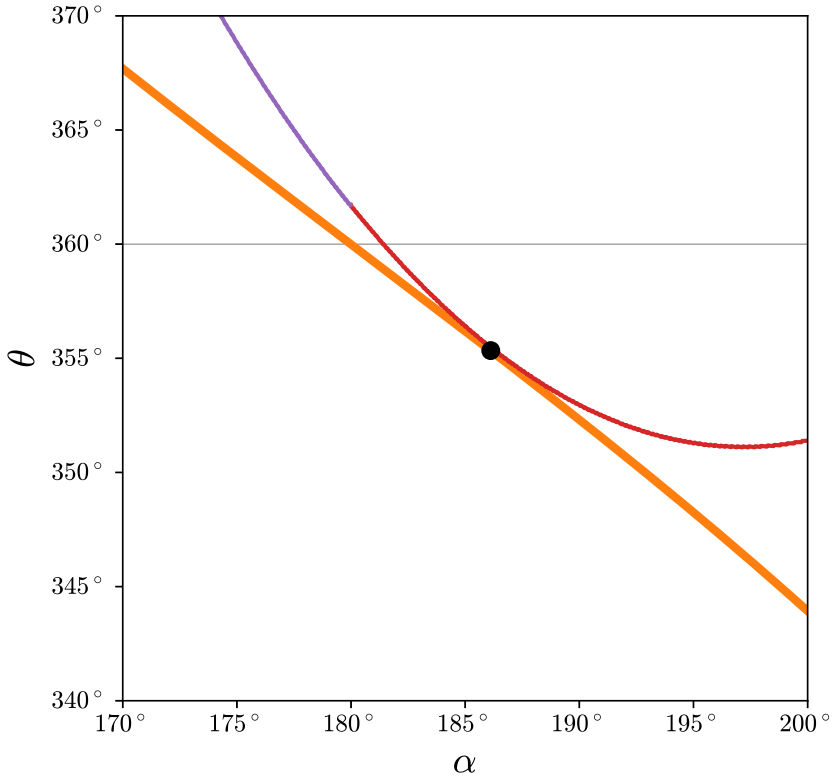

FIG. 6. This plot shows the boxed region identified in the second panel of Fig. 5 in higher resolution. Under the conditions of $\delta = 0.20$ and $\theta_0 = 15°$ there is a stable solution in the neighborhood of $\alpha = 180°$ where the LHS and RHS of Eq. 14 are tangent to each other.

the mathematical complexity of the stability condition that arises due to the many ways in which dependence on α enters through both the LHS and RHS of Eq. 14. Instead of providing a mathematical proof, the general existence of stable solutions is proved with an example. The boxed region in the right panel of Fig. 5 identifies a solution for the case of $\delta = 0.39$ and $\theta_0 = 15°$. This region is expanded in Fig. 6, which clearly shows that the two curves are tangent to each other under these conditions. It follows that this solution is stable with respect to small deviations in α and, therefore, that stable solutions exist for the second family of intercept solutions. It is left as an exercise for the reader to prove whether there exist stable fast-intercept solutions.

VI. RENDEZVOUS

The conditions on the thrust required for rendezvous can be derived from the equations of motion or from symmetry arguments. We follow the latter path here. Interception with a solution from the second family of intercept points occurs at a point of mixed symmetry in the orbit, where the angular velocity is that same but the radial velocity is reversed compared to the situation just following engine burn. Such a velocity could have been produced with a thrust of magnitude δ at an angle of $-\alpha$. The thrust required to complete rendezvous must be equal and opposite to the velocity differential at interception, and it therefore follows that the rendezvous maneuver requires a thrust of magnitude δ at an angle of $\pi - \alpha$. In contrast, it was shown in Ref. [5] that the thrust angle required for rendezvous for the first family of solutions is $\pi + \alpha$.

VII. CONCLUSIONS

The analysis presented in this work concludes the intercept problem that was originally presented in Ref. [5] by demonstrating how the method of solution can be extended to the second family of intersection locations. The general intercept condition that was derived here is a transcendental equation, which achieves a rather complex dependence on the control parameters through the relationships describing the eccentricity and orbital phase. In addition to presenting a method for finding solutions for the second family of intercept locations, this work showed the existence of fast-intercept solutions within one orbit of the chaser, and proved the existence of stable solutions through an example with $\delta = 0.39$ for $\theta_0 = 15°$. Furthermore, the general intercept condition derived here encompasses the first family of intercept solutions when it is limited to intercept at $\theta_x = 2\pi$.

It is certainly the case that in most situations involving mission planning for intercept and rendezvous maneuvers neither the thrust magnitude nor the time to intercept are completely arbitrary, and it is likely that multiple constraints are relevant. It may be that the best method for finding solutions is to further limit the solution space generated by a single constraint. For example, if one were also interested in the time to intercept, that information could be calculated for each of the orbits and presented as auxiliary information, similar to the θ_x curve of Fig. 4. A constraint of limited fuel is highly relevant in many contexts

and, compared to the Lambert problem, has the benefit that it is natural to visualize a thrust vector that is constant in magnitude and varies only in direction, which is a central feature of the intercept problem considered here. The entirety of this intercept problem, first through the work of Ref. [5] and followed by this work, presents a series of intuition-building exercises that demonstrate how, even for introductory problems, complexity quickly arises as a problem is extended, but can nonetheless be greatly simplified when viewed in particular ways. There are, of course, many other challenging problems that could be further examined from this point, including the mathematical expression for the stability condition associated with Eq. 14, the existence of stable fast-intercept maneuvers, initial orbits that are not circular, and initial conditions that are not co-orbital.

AUTHOR DECLARATIONS

The authors have no conflicts to disclose.

---

[1] J. L. Lagrange. *Mécanique Analytique, Vol. II.* Académie des Sciences, Paris, 1788.

[2] C. F. Gauss. *Theory of the motion of the heavenly bodies moving about the Sun in conic sections: a translation of Gauss's "Theoria motus."*. Little, Brown and Co., 1857.

[3] I. R. Gatland. Gravitational orbits and the Lambert problem. *American Journal of Physics*, 90(3):177, 2022.

[4] A. M. Capece and J. L. Gazley. The Hohman transfer as an application for teaching introductory physics. *American Journal of Physics*, 89(11):1002, 2021.

[5] E. M. Edlund. Interception and rendezvous: An intuition-building approach to orbital dynamics. *American Journal of Physics*, 89:559, 2021.

[6] P. R. Blanco and C. E. Mungan. High-speed escape from a circular orbit. *American Journal of Physics*, 89(1):72, 2021.

[7] L. M. Smallwood, D. M. Katz, and M. W. Richmond. Near earth objects: A brief review and a student project. *American Journal of Physics*, 72(2):264, 2004.

[8] NASA. Planetary defense coordination office, 2022. URL `https://www.nasa.gov/planetarydefense/overview`.

[9] A. F. Chang, A. S. Rivkin, P. Michel, J. Atchison, O. Barnouin, L. Benner, N. L. Chabot, C. Ernst, E. G. Fahnestock, M. Keuppers, P. Pravec, E. Rainey, D. C. Richardson, A. M. Stickle, and C. Thomas. AIDA DART asteroid deflection test: planetary defense and science objectives. *Planetary and Space Science*, 157:104, 2018.

[10] T. Pultarov. Astroscale's space junk removal satellite aces 1st orbital test, 2021. URL `https://www.space.com/astroscale-first-space-junk-capture-demonstration`.

[11] W. J. Hennigan. Exclusive: Strange Russian spacecraft shadowing U.S. spy satellite, general says, 2020. URL `https://time.com/5779315/russian-spacecraft-spy-satellite-space-force/`.

[12] R. D. H. Warburton and J. Wang. Analysis of asymptotic projectile motion with air resistance using the Lambert W function. *American Journal of Physics*, 72:1404, 2004.

[13] B. C. Reed. A guide to the literature of the finite rectangular well. *American Journal of Physics*, 89:529, 2021.

[14] A. A. Othman, M. de Montigny, and F. Marsiglio. The Coulomb potential in quantum mechanics revisited. *American Journal of Physics*, 85:346, 2017.

[15] F. Szmulowicz. Analytical, graphical, and geometric solutions for photonic band gaps. *American Journal of Physics*, 72:1392, 2004.

[16] J. R. Mendonça. Electromagnetic surface wave propagation in a metallic wire and the Lambert W function. *American Journal of Physics*, 87:476, 2019.

[17] H. Goldstein, C. P. Poole, and J. Safko. *Classical Mechanics*. Pearson, 2011.